Phased Array Antenna Calibration and Pattern Prediction Using Mutual Coupling Measurements

HERBERT M. AUMANN, MEMBER, IEEE, ALAN J. FENN, SENIOR MEMBER, IEEE, AND FRANK G. WILLWERTH

Abstract—**Large phased array antennas are commonly tested using far-field or near-field sources. While these source arrangements are well suited to ground testing, they may be difficult to implement in airborne or spaceborne applications. A technique which utilizes the inherent mutual coupling in an array to both calibrate and predict the radiation patterns of a phased array antenna is investigated. The only restriction of the technique is that the ability to transmit and receive with pairs of the array elements is required. The theory associated with array mutual coupling and its relationship to both array calibration and array patterns is discussed. The design of a test bed phased array antenna is covered. The mutual coupling technique (MCT) is used experimentally to calibrate the test array as well as to predict the array radiation patterns. It is shown that the results obtained by MCT are in good agreement with conventional far-field measurements.**

I. Introduction

LARGE PHASED ARRAY antennas are commonly suggested for airborne or spaceborne [1] applications. To achieve desired radiation pattern performance levels in flight, such as main beam shape and low sidelobes, it is necessary for the array to be well calibrated. By well calibrated, it is meant that strict amplitude and phase tolerances are maintained at each array element. Ground-based phased arrays are typically calibrated using external far-field or near-field test sources. However, for airborne or space-based antenna applications, external calibration sources may be impractical or difficult to implement. Thus, alternate array calibration techniques are desirable.

An example of external source array calibration is discussed in [2]. The authors used a planar near-field scanner to calibrate a 96-element L-band planar phased array. A receive probe was positioned sequentially in front of each radiating element with all other array elements terminated in matched loads. The amplitude and phase of each radiating element were measured as the antenna-element RF weights (modules) were cycled through their amplitude and phase states. A desired array illumination is then achieved by selecting appropriate amplitude and phase settings from the above near-field measured data.

This paper develops mathematically and demonstrates experimentally a calibration and radiation pattern measurement technique which takes advantage of the inherent mutual coupling in an array, by transmitting and receiving between all adjacent pairs of radiating elements through two independent beamformers (corporate feeds). Thus, this technique utilizes an internal calibration source. It is shown that after calibrating in this fashion, it is possible to measure the array illumination and, thus, compute the antenna radiation pattern.

The paper is organized in the following manner. In Section II, a theory for array calibration and far-field radiation pattern prediction using mutual measurements is developed. Section III discusses the design of a displaced phase center antenna (DPCA) used during experimental evaluation of the array calibration and pattern prediction method. Comparisons of the experimental results, of direct far-field and mutual coupling calibration and radiation patterns, are given in Section IV. It is shown that the measured data for the mutual coupling technique (MCT) is in good agreement with the direct far-field data.

Manuscript received April 7, 1987; revised July 26, 1988. This work was supported by the U.S. Department of the Air Force.

The authors are with the Lincoln Laboratory, Massachusetts Institute of Technology, P.O. Box 73, Lexington, MA 02173.

IEEE Log Number 8927674.

II. Theory

A. Array Illumination and Radiation Patterns

Consider the radiation pattern computation for an N-element array antenna including mutual coupling effects. In a passively terminated array as shown in Fig. 1, where a single element is driven (e.g., element m) and the surrounding elements are terminated, in the generator impedance, let the mth element far-field vector radiation pattern be denoted by $\mathbf{p}_m(\theta, \phi)$. For the entire array transmitting, with mutual coupling, the array pattern is expressed as [3]

$$\mathbf{P}_a(\theta, \phi) = \sum_{m=1}^{N} \mathbf{p}_m(\theta, \phi) v_m e^{j\psi_m} \tag{1}$$

where v_m is the complex excitation coefficient (or illumination) of the mth element,

$$\psi_m = \frac{2\pi}{\lambda} \sin\theta (x_m \cos\phi + y_m \sin\phi), \tag{2}$$

λ is the wavelength, (x_m, y_m) are the rectangular coordinates for the mth element and (θ, ϕ) are standard spherical coordinates for the observation angles. In a large, uniform array it can be assumed that the element radiation patterns are identical and do not vary with element position, that is,

$$\mathbf{P}_1 = \mathbf{p}_2 = \cdots = \mathbf{p}_N = \mathbf{p}_e(\theta, \phi), \tag{3}$$

0018-926X/89/0700-0844$01.00

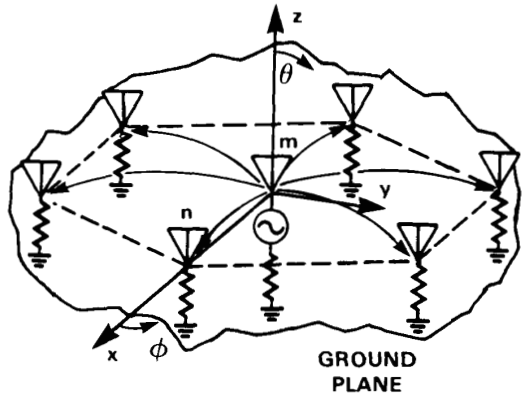

Fig. 1. Two-dimensional passively terminated antenna array with mth element driven. Curved arrows originating from element m represent mutual coupling to surrounding elements.

where $\mathbf{p}_e(\theta, \phi)$ is referred to as the embedded element pattern. Using (3) in (1) the array pattern expression then simplifies to

$$\mathbf{p}_a(\theta, \phi) = \mathbf{p}_e(\theta, \phi) \sum_{m=1}^{N} v_m e^{j\psi m}. \tag{4}$$

The objective of array calibration is to compensate for hardware imperfections and permit the above desired excitation coefficients v_m to be implemented. Additionally, if the element pattern is known, measurement of the array excitation permits construction of array patterns.

B. Array Self-Calibration

In this section, array mutual coupling [3], [4] is used to arrive at a method for calibrating an array with internal sources; hence, the term self-calibration is appropriate.

Calibration of phased array modules can be broken up into two parts, that is, determination of the module insertion attenuation and phase, and determination of the module attenuator and phaser transfer functions. Depending on the hardware configuration, separate transmit and receive parameters may have to be determined. All of these calibrations can be performed by mutual coupling measurements.

In order to carry out the mutual coupling measurements described below, a phased array must meet two requirements. The first requirement, which has already been mentioned, is that the array elements are uniformly spaced and have identical, symmetric radiation patterns. The second requirement is that the array have an ability to transmit with one element and simultaneously receive with another element. Ordinarily, this second requirement implies separate transmit and receive beamforming networks.

Ideally, in a large, uniform, planar array of thousands of elements, the mutual coupling (defined as the ratio of received to transmitted signal) between pairs of adjacent elements is invariant to the pair position. While the free space mutual coupling is indeed position invariant, the measured coupling between two adjacent elements in a phased array includes effects of feed lines, power combiners/dividers, and transmit/receive modules and is clearly sensitive to hardware differences.

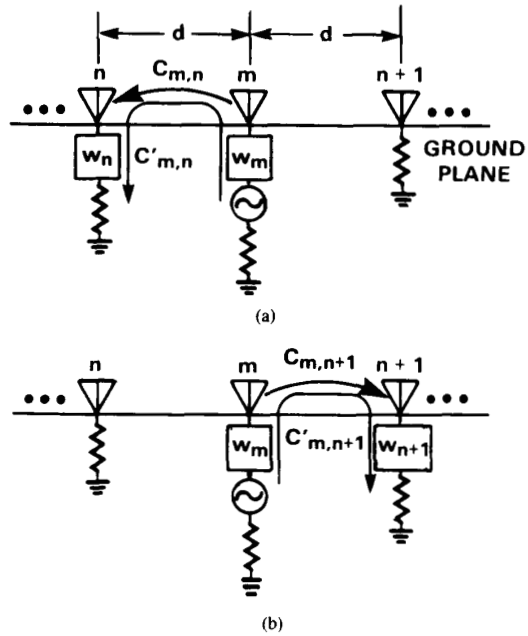

Fig. 2. Comparison of free space mutual coupling and transfer function which includes free space coupling and feedline/module effects. (a) Coupling and transfer function for m, nth elements (b) Coupling and transfer function for m, $n + 1$th elements.

This can be seen in the example of a linear array depicted in Fig. 2, where C denotes free space mutual coupling, and C' is the transfer function which includes the free space mutual coupling contribution plus feedline and module effects. If the element patterns are symmetrical and the elements are equidistant, then

$$C_{m,n} = C_{m,n+1}. \tag{5}$$

However, due to intentional or unintentional hardware differences, the measured transfer functions[1] will not be equal, that is,

$$C'_{m,n} \neq C'_{m,n+1}. \tag{6}$$

It is immediately noticed that the path through the transmitting element m is common to both measurements. Hence any differences in $C'_{m,n}$ and $C'_{m,n+1}$ are due to differences between the receiving element signal paths n and $(n + 1)$ alone.

The measured transfer function can be considered to be made up of an attenuator and phaser setting in the transmit and receive modules, denoted respectively by the complex quantities $w_m(i)$ and $w_n(j)$, where i and j refer to the ith and jth complex state, and the combined effects of attenuation and phase delay in the RF cables, connector and power dividers, denoted by the complex quantities u_m and u_n. Also combined within u_m and u_n are the insertion attenuation and phase of the attenuator and phase shifters when they are set to their digital references, or zero state. Thus, the measured transfer function

[1] The primes will denote measured quantities, or quantities calculated directly from measured quantities.

when transmitting from the mth element and receiving with the nth element is evaluated by the following expression:

$$C'_{m,n} = w_m u_m C_{m,n} w_n u_n. \tag{7}$$

Similarly, upon transmitting from the mth element to the $(n+1)$th element, it is clear that

$$C'_{m,n+1} = w_m u_m C_{m,n+1} w_{n+1} u_{n+1}. \tag{8}$$

Since it is assumed that the elements are symmetrical and equidistant, application of (5) to the ratio of (7) to (8) yields

$$W'_{n+1} = \frac{C'_{m,n}}{C'_{m,n+1}} = \frac{w_n u_n}{w_{n+1} u_{n+1}}. \tag{9}$$

In particular, by definition, in the zero state, $i = j = 0$,

$$w_n(0) = w_{n+1}(0) = 1$$

then (9) reduces to

$$W'_{n+1}(0) = \frac{u_n}{u_{n+1}}, \qquad n = 0, 1, \cdots, N-1. \tag{10}$$

The quantity W'_{n+1} is the ratio of the complex insertion of the nth to $(n+1)$th element signal paths. This ratio, when used as a complex multiplier, makes the signal received by element $(n+1)$ look like the signal received by element n. Henceforth, any measurement at element $(n+1)$ will be multiplied by $W'_{n+1}(0)$.

In order to extend this concept, consider a larger, two-dimensional array as shown in Fig. 3. Let it be assumed that element $(m+1)$ is equidistant from elements $(n+1)$ and $(n+2)$. By transmitting from element $(m+1)$ and receiving first with element $(n+1)$ and then with element $(n+2)$, $C'_{m+1,n+1}$ and $C'_{m+1,n+2}$ can be measured as described in Section IV-A. Now, calculate

$$W'_{n+2}(0) = \frac{C'_{m+1,n+1} W'_{n+1}(0)}{C'_{m+1,n+2}} \tag{11}$$

which is equivalent to

$$W'_{n+2}(0) = \frac{u_n}{u_{n+2}}, \tag{12}$$

or referenced to the first element

$$W'_{n+2}(0) = \prod_{i=1}^{n+1} \frac{u_i}{u_{i+1}} = \frac{u_1}{u_{n+2}}. \tag{13}$$

Note that $1/W'_{n+2}(0)$ is the insertion attenuation and phase of the $(n+2)$th element relative to the first, or reference element. The relative insertion measurements can be further refined by averaging. For example, for the elements shown in Fig. 3, there will be in general, two equidistant nearest neighbors. Thus, the elements m and k are equidistant from n and $(n+1)$. Hence, W'_{n+1} could have been determined also as

$$W'_{n+1}(0) = \frac{C'_{k,n}}{C'_{k,n+1}} \tag{14}$$

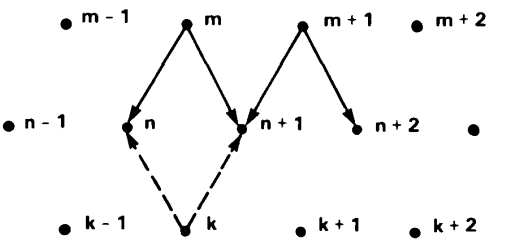

Fig. 3. Two-dimensional array with hexagonal lattice. The arrows represent the mutual coupling or transfer function between two elements.

which mathematically yields the same result as (10). Of course, in an actual measurement, the results will be slightly different. A more precise measurement of W'_{n+1} would therefore be the average of the two sets of measurements, or,

$$W'_{n+1}(0) = \frac{1}{2}\left(\frac{C'_{k,n}}{C'_{k,n+1}} + \frac{C'_{m,n}}{C'_{m,n+1}}\right). \tag{15}$$

In a hexagonal grid array this concept can be expanded to include the six equidistant nearest neighbors, that is elements $m, n, k, m+1, n+2, k+1$ are equidistant from element $(n+1)$.

Mutual coupling measurements can also be used to determine the transfer function of each element in the jth state relative to the zero state. Noting again that $w_{n+1}(0) = 1$, the ratio of (9) and (10) yields

$$\frac{W'_{n+1}(j)}{W'_{n+1}(0)} = \frac{w_{n+1}(j)}{w_{n+1}(0)} = w_{n+1}(j). \tag{16}$$

The mutual coupling calibration technique described in this paper cannot, of course, correct for element radiation pattern variations due to asymmetry in the elements or uncertainty in the element position. In fact, for this approach to be valid, it must be assumed that the element pattern variations do not limit the ability to calibrate the array to a desired level of amplitude and phase error or a particular performance quantity (such as sidelobe level). An analysis of the effects of element pattern variations in a finite array is beyond the scope of this paper.

C. Array Radiation Pattern Prediction

Let it be assumed that the array has been calibrated by the above method, and the desired array excitation for the nth element is given by the complex coefficient v_n. To implement the excitation function and correct for insertion attenuation and phase differences between elements, the array module attenuator and phaser have to be set to some state i such that

$$w_n(i) = v_n W'_n(0). \tag{17}$$

A neighboring element, say $(n+1)$, will have to be set to a different state j, such that

$$w_{n+1}(j) = v_{n+1} W'_{n+1}(0). \tag{18}$$

However, due to quantization effects and for other reasons, the array excitation will not be perfectly implemented. As in

(9), from measurements the ratio

$$\frac{C'_{m,n}}{C'_{m,n+1}}=\frac{w_n(i)u_n}{w_{n+1}(j)u_{n+1}}=\frac{v_n W'_n(0)u_n}{v_{n+1}W'_{n+1}(0)u_{n+1}} \tag{19}$$

can be determined.

Now, from (13), $W'_n(0) = u_1/u_n$ and $W'_{n+1}(0) = u_1/u_{n+1}$. Hence, it follows that

$$\frac{C'_{m,n}}{C'_{m,n+1}}=\frac{v_n}{v_{n+1}} \tag{20}$$

is the ratio of the element excitations. If referenced to the first measurement

$$E'_{n+1}=\prod_{i=1}^{n}\frac{C'_{m,i}}{C'_{m,i+1}}=\frac{v_1}{v_{n+1}}. \tag{21}$$

The reciprocal of the product of measurements, $1/E'_n$, is a measurement of the actually applied excitation function relative to a reference element.

The fact that E'_n is a product of measurements indicates that some consideration should be given to the choice of the reference element location and the path taken to the element n in order to minimize cumulative error build up. This is particularly true in cases when a severe array taper has been applied.

If a typical embedded element pattern, $p'_e(\theta, \phi)$, can be determined, for example by far-field measurements, then the array radiation pattern can be computed from

$$P'_a(\theta, \phi)=p'_e(\theta, \phi)\sum_{m=1}^{N}\frac{1}{E'_m}e^{j\psi_m} \tag{22}$$

where ψ_m is given by (2).

The efficacy of (13) and (16) for carrying out phased array calibrations, and (2), (21), and (22) for determining phased array antenna patterns will be considered in Section IV.

III. Test Array Description

As part of an effort to evaluate the displaced phase center antenna concept, a 96-element phased array was developed. The basic characteristics of the test array are shown in Table I. This array was particularly suitable for making mutual coupling measurements because of the omnidirectional monopole elements and availability of two corporate feeds. The dimensional layout of the 96-element test array is shown in Fig. 4. In order to provide the desired scan volume without grating lobes, the monopole elements were mounted on a hexagonal grid with 0.55 wavelength spacing at the center frequency.

A block diagram of the modules and beamformer connections is shown in Fig. 5. The beamformer is arranged in quadrants to permit sum and difference signals to be formed. The signals from the module A channels are combined by six 4:1 combiners in each quadrant, followed by two 12:1 combiners for the two upper and two lower quadrants. A final 2:1 combiner generates the beam A signal. An identical beamforming network combines the signals from the module B channels. Coaxial cables were used as the feedlines connecting the modules to the power dividers.

TABLE I
TEST ARRAY CHARACTERISTICS

96 (8 × 12) active elements, monopole radiators
Frequency band 1.2–1.4 GHz
Two corporate feed DPCA beams
Six-bit phasers (64 states), uniform 5 5/8 degrees steps
7-step attenuators, nonuniform steps
(0 1.3 2.8 4.6 6.8 10.0 > 55 dB)
Conical scan to 60° with fixed broadside null vertical polarization

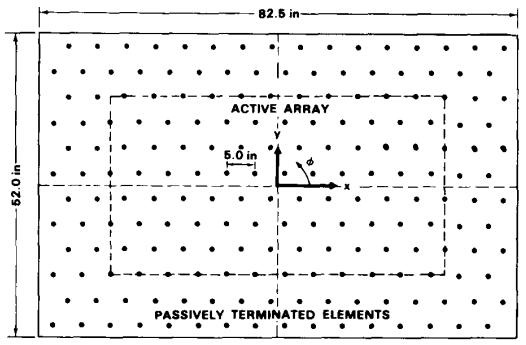

Fig. 4. 96-element test array layout.

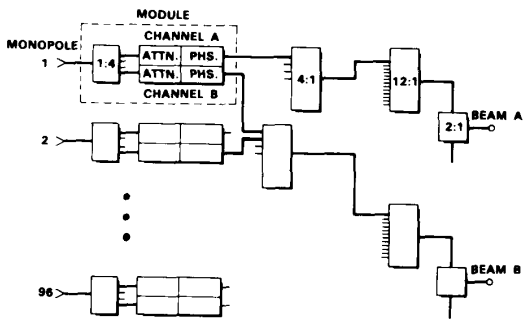

Fig. 5. Test array beamformer block diagram.

A photograph of one of the test array modules is shown in Fig. 6. The module contains two digitally controlled 360° six-bit diode phase shifters and two digitally controlled 0–10 dB 6 step + off (>55 dB) attenuators. By selectively turning off modules, the active area of the array can be shifted, effecting a phase center displacement.

The antenna radiating elements selected for the test array were thin cylindrical monopoles. In an array [5], the monopole has wide-scan coverage beginning at about 30° from broadside with azimuthally omnidirectional vertical polarization, and has a deep null at broadside as shown in Fig. 7. Such a radiating element is desirable for spaceborne applications [1].

A 100 ft ground reflection range was used for far-field calibrations and measurements. These measurements served as reference for similar measurements based on mutual coupling. A photograph of the test array located inside the radome of the far-field range is shown in Fig. 8.

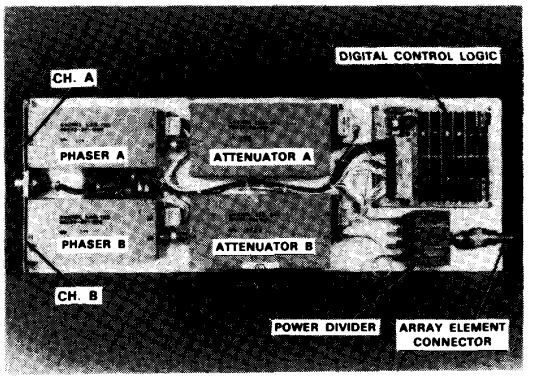

Fig. 6. Photograph of dual-channel test array module.

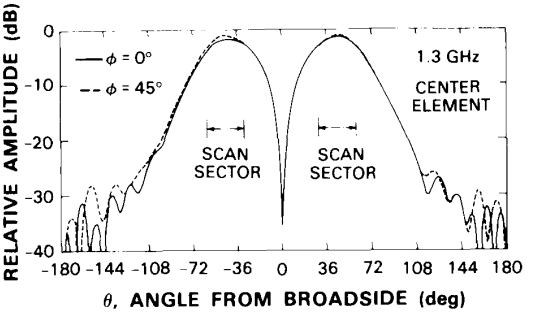

Fig. 7. Measured center element radiation pattern for an 11-row by 11-column monopole array [5].

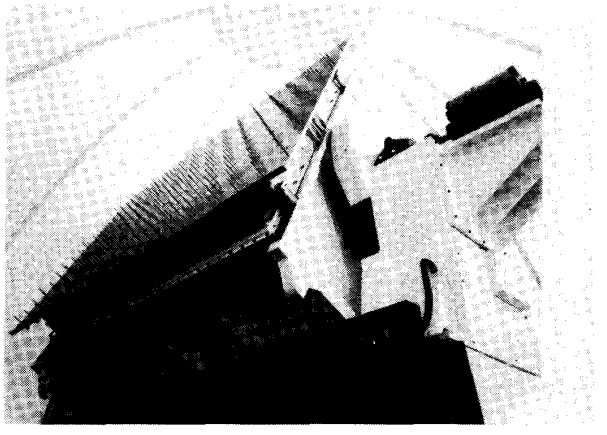

Fig. 8. Photograph of 96-element test array inside radome of far-field range.

IV. Experimental Results

A. Phased Array Calibration by Mutual Coupling Measurements

The measurement techniques used in either a near-field or far-field antenna range could, in principle, be used for ground testing a DPCA phased array. However, they are really not amenable to testing and calibrating a system in-flight. Phased array calibration and testing by mutual coupling measurements appears to offer a viable alternative.

It was desired to investigate experimentally the mutual coupling technique using the previously mentioned test array. Validation of the calibrations is made by comparison to standard far-field measurements.

Mutual coupling measurements require an ability to transmit and receive at the same time. This is not a problem in the low power, passive test array described here. In a fielded radar system, additional hardware and protective interlocks would be required. However, as will be demonstrated, mutual coupling measurements offer significant advantages, even for ground testing. They permit complete module attenuation and phase calibration of the installed module. Since an external source is not required for making mutual coupling measurements, the array can be positioned so as to minimize reflections from surrounding objects. Pointing the array straight up is an advantageous position for reducing ground multipath. In the measurements described below, the test array surface was parallel to and approximately 15 ft above the ground.

The measurement technique is best illustrated by referring to the test array block diagram in Fig. 5. The 96-element test array already contains two independent beamforming networks which allows a simultaneous transmit and receive function to be readily implemented. Since the experimental measurements were made at very low power levels, no protective hardware was required. Mutual coupling measurements were made by arbitrarily designating the attenuators and phasers of beam B to form the transmit beam, and the attenuators and phasers of beam A to form the receive beam. The amplitude and phase of a signal at point A relative to point B is then measured, with all elements terminated except for one transmit and one receive element.

In general, mutual coupling calibration is a two-step process. First, the transmit elements are calibrated to provide a desired, in this case uniform amplitude, array illumination. This is done exactly as described in Section II-B, except that the words "transmit" and "receive" are interchanged. Next, the receive element calibration is performed. Since the test array modules are passive, reciprocity would allow the first step to be eliminated, thus simplifying the calibration process. However, this fact was not taken advantage of because such a simplification would probably not be possible in a fielded system.

Fig. 9 shows the module insertion phase for the 96-elements of the test array as determined by far-field measurements (range is 100 ft, scan angle is 40 degrees) and by mutual coupling measurements. For certain elements, there are large phase differences between modules. These differences are due to the use of 2:1 power dividers from different manufacturers in front of those modules. The differences could have been corrected by trimming cables, however, this was felt to be unnecessary because of subsequent calibration in software. Here, the differences were advantageous in illustrating the similarity between measurements obtained on the far-field range and measurements obtained by mutual coupling.

A comparison of the far-field and mutual coupling insertion attenuation measurements shown in Fig. 10 does not show any trend, however, the standard deviation of the mutual coupling determined insertion attenuation (0.3 dB) is considerably

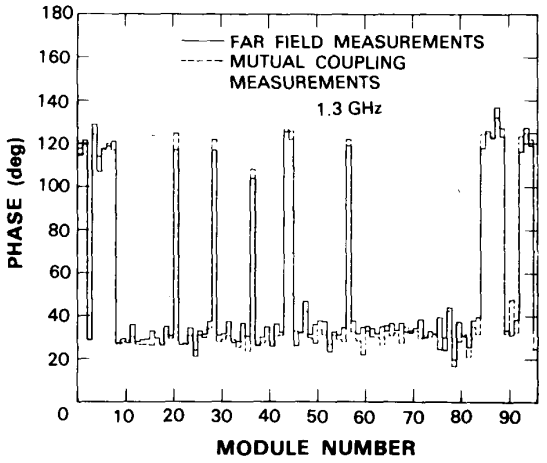

Fig. 9. Test array module insertion phase before calibration, obtained from mutual coupling measurements and direct far-field measurements.

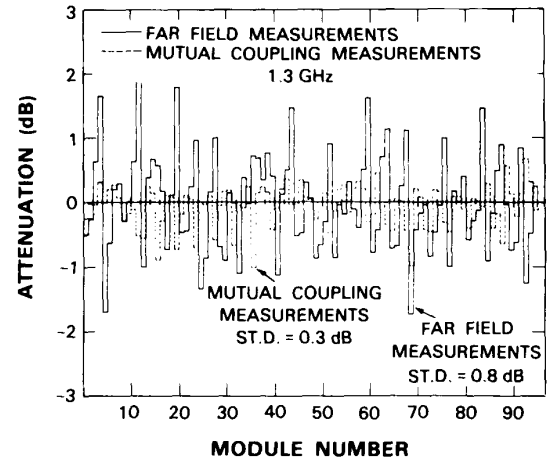

Fig. 10. Test array module insertion attenuation, before calibration, obtained from mutual coupling measurements and direct far-field measurements.

smaller than that of the far-field determined attenuation (0.8 dB). Since the mutual coupling determined standard deviation of 0.3 dB is more consistent with the specifications and bench measurements of individual modules, it is assumed that the far-field measurements were affected by multipath.

Having calibrated the transmit elements, the insertion attenuation and phase of the receive elements can now be measured. For a given receive element, a transmission is made from each of the six surrounding, equidistant nearest neighbor elements. The measurements of the receiving element signal are scaled by the appropriate transmit calibration constant. As suggested by (15), the average of the six measurements yields the receive element insertion attenuation and phase.

B. Mutual Coupling Derived Antenna Pattern Measurements

Obtaining antenna patterns from mutual coupling measurements is in many ways similar to the calibration procedure. In order to obtain a receive antenna pattern, the receive elements must first be calibrated in the manner described in Section II-B. Then, the attenuators and phase shifters in each module are set to the desired beamforming commands and the calibration procedure is repeated. By chosing the reference element to be in the center of the array, cumulative measurement error build-up was minimized.

As described in Section II-C, the far-field pattern can be synthesized by setting in (4)

$$\frac{v_m}{v_1} = 1/E'_m,$$

and evaluating ψ_m in (2) from the well-known location (x_m, y_m) of the mth element. An average embedded monopole pattern $p_e(\theta, \phi)$ can be obtained by using a representative monopole pattern determined by separate far-field measurements.

Comparisons of patterns obtained from mutual coupling measurements with conventional far-field measurements are shown in Figs. 11 and 12. Fig. 11 shows a test array azimuth pattern cut with uniform illumination, and Fig. 12 shows a pattern with a 10 dB cosine edge taper (no pedestal). In both cases, a very good match is obtained for the main lobe and the first sidelobes. There are some differences in the far sidelobes at the -30 dB level, which can be attributed to differences in the multipath environment and the assumption of identical element patterns.

Once the element excitations for a particular scan angle have been determined, two-dimensional patterns can also be obtained from (4). Fig. 13 shows such a pattern in u, v space ($u = \sin\theta \cos v = \sin\theta \sin\phi$) for the test array with -10 dB edge illumination. No attempt was made to validate this two-dimensional pattern using direct far-field measurements; this would have required an enormous measurement effort.

V. Conclusion

This paper has addressed a technique which uses mutual coupling measurements for calibration of large phased arrays. The technique uses an internal test source and so the phrase "array self-calibration" is appropriate to these measurements. The mutual coupling technique is applicable to a phased array having dual beamformers with modules that can be used to select transmit/receive element pairs within the array. This calibration method enforces invariance of the mutual coupling through all adjacent-element channels (or signal paths) to provide uniform illumination. For a desired array illumination, errors due to array weight quantization are then measured by a second application of the MCT. Array radiation patterns can be calculated from the measured array illumination, the known array element positions, and a known embedded element pattern.

An experimental investigation of array mutual coupling has produced good agreement with conventional far-field calibration and pattern measurements of a 96-element corporate fed phased array antenna. Two-dimensional radiation patterns are readily achieved, using MCT, as was demonstrated. The technique may be applicable to calibrating phased arrays in flight. Although more conventional arrays such as dipole or

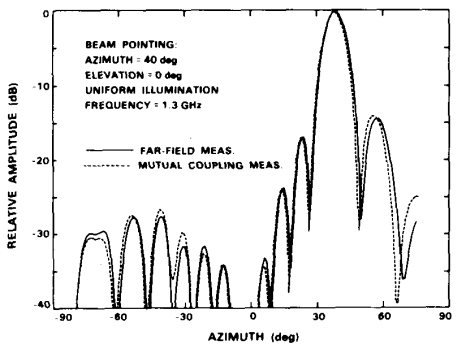

Fig. 11. Comparison of test array far-field radiation pattern obtained from the mutual coupling technique and direct far-field measurements, uniform illumination.

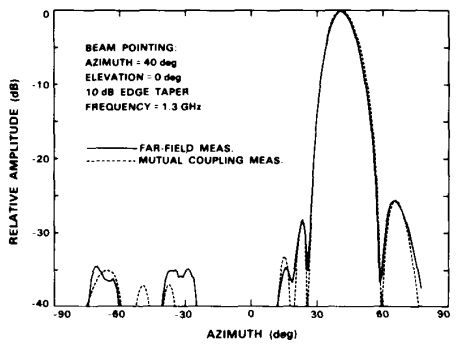

Fig. 12. Comparison of test array far-field radiation pattern obtained from the mutual coupling technique and direct far-field measurements, -10 dB cosine taper illumination.

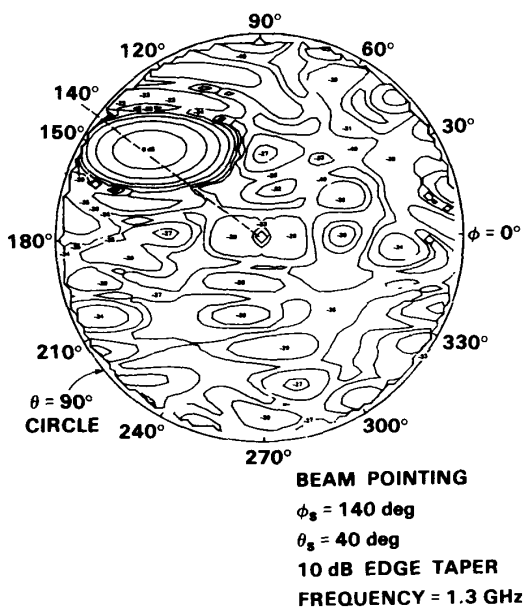

Fig. 13. Mutual coupling derived two-dimensional antenna pattern in u, v space.

waveguide arrays were not considered in this paper, it is expected that the MCT is applicable for such array calibration and pattern prediction.

References

[1] E. J. Kelly and G. N. Tsandoulas, "A displaced phase center antenna concept for space based radar applications," in *Proc. IEEE Eascon*, Sept. 1983, pp. 141–148.

[2] A. J. Fenn, F. G. Willwerth, and H. M. Aumann, "Displaced phase center antenna near field measurements for space based radar applications," in *Phased Arrays 1985 Symp. Proc.*, RADC-TR-85-171 in-house Rep., ADA-169316, pp. 303–318, Aug. 1985.

[3] J. L. Allen and B. L. Diamond, "Mutual coupling in array antennas," Lincoln Lab., Massachusetts Inst. Technol., Lexington, MA, Tech. Rep. 424, Oct. 4, 1966, DDC 648153.

[4] N. Amitay, V. Galindo, and C. P. Wu, *Theory and Analysis of Phased Array Antennas*. New York: Wiley, 1972.

[5] A. J. Fenn, "Theoretical and experimental study of monopole phased array antennas," *IEEE Trans. Antennas Propagat.*, vol. AP-33, no. 10, pp. 1118–1126, Oct. 1985.

Herbert M. Aumann (S'64–M'67) received the B.S. degree in electrical engineering from the University of Idaho in 1965, the M.S. degree from Colorado State University in 1967, and the Ph.D. from the University of Wisconsin in 1973.

From 1967 to 1969 he was an Instructor in the Department of Electrical Engineering at the University of Wisconsin. In 1973, he joined the Massachusetts Institute of Technology Lincoln Laboratory, working in various areas of radar signal processing. He is currently involved in space-based radar technology development.

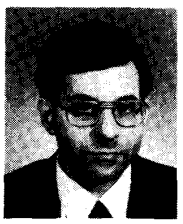

Alan J. Fenn (S'74–M'75–SM'87) received the B.S. degree from the University of Illinois, Chicago Circle, in 1974, and the M.S. and Ph.D. degrees from The Ohio State University, Columbus, in 1976 and 1978, respectively, all in electrical engineering.

From 1974 to 1978 he was a Graduate Research Associate at The Ohio State University Electro-Science Laboratory. He was a Senior Engineer at Martin Marietta Aerospace, Denver, CO, from 1978 to 1981 where he was involved in broad-band antenna research and development. In 1981 he became a Staff Member at the Massachusetts Institute of Technology Lincoln Laboratory. He is currently in the space radar technology group in which his research has involved phased array antenna design, adaptive nulling studies, and antenna and radar cross section measurements.

Frank G. Willwerth received the B.S. degree in electrical engineering from Tufts University, Medford, MA, in 1966, and subsequently did graduate work at Tufts University and at the Massachusetts Institute of Technology.

From 1966 to 1968 he was with Sylvania Electric Company where he was engaged in microwave integrated circuit development. In 1968 he joined the Massachusetts Institute of Technology Lincoln Laboratory, where he is currently a staff member in the space radar technology group. His research has involved antenna design, near field measurements, and adaptive nulling receiver design.